Remote Sens. **2013**, *5*, 254-273; doi:10.3390/rs5010254

OPEN ACCESS

Remote Sensing

ISSN 2072-4292

www.mdpi.com/journal/remotesensing

Article

Retrieving the Bioenergy Potential from Maize Crops Using Hyperspectral Remote Sensing

Thomas Udelhoven [1,2,*], Philippe Delfosse [2], Christian Bossung [1], Franz Ronellenfitsch [2], Frédéric Mayer [2], Martin Schlerf [2], Miriam Machwitz [2] and Lucien Hoffmann [2]

[1] Department of Environmental Remote Sensing and Geoinformatics, Trier University, D-54286 Trier, Germany; E-Mail: bossung@uni-trier.de

[2] Department Environment and Agro-Biotechnologies, Centre de Recherche Public-Gabriel Lippmann, 41, rue du Brill, L-4422 Belvaux, Luxembourg; E-Mails: delfosse@lippmann.lu (P.D.); ronellen@lippmann.lu (F.R.); mayer@lippmann.lu (F.M.); schlerf@lippmann.lu (M.S.); machwitz@lippmann.lu (M.M.); hoffmann@lippmann.lu (L.H.)

* Author to whom correspondence should be addressed; E-Mail: udelhoven@uni-trier.de; Tel.: +49-651-201-4513; Fax: +49-651-201-3815.

Received: 20 November 2012; in revised form: 4 January 2013 / Accepted: 4 January 2013 / Published: 15 January 2013

Abstract: Biogas production from energy crops by anaerobic digestion is becoming increasingly important. The amount of biogas that can be produced per unit of biomass is referred to as the biomethane potential (BMP). For energy crops, the BMP varies among varieties and with crop state during the vegetation period. Traditional ways of analytical BMP determination are based on fermentation trials and require a minimum of 30 days. Here, we present a faster method for BMP retrievals using near infrared spectroscopy and partial least square regression (PLSR). PLSR prediction models were developed based on two different sets of spectral reflectance data: (i) laboratory spectra of silage samples and (ii) airborne imaging spectra (HyMap) of maize canopies under field (*in situ*) conditions. Biomass was sampled from 35 plots covering different maize varieties and the BMP was determined as BMP per mass (BMP_{FM}, Nm^3 biogas/t fresh matter (Nm^3/t FM)) and BMP per area (BMP_{area}, Nm^3 biogas/ha (Nm^3/ha)). We found that BMP_{FM} significantly differs among maize varieties; it could be well retrieved from silage samples in the laboratory approach (R_{cv}^2 = 0.82, n = 35), especially at levels >190 Nm^3/t. In the *in situ* approach PLSR prediction quality declined (R_{cv}^2 = 0.50, n = 20). BMP_{area}, on the other hand, was found to be strongly correlated with total biomass, but could not be satisfactorily predicted using airborne HyMap imaging data and PLSR.

Keywords: agriculture; bioenergy; biomethane potential; hyperspectral remote sensing

1. Introduction

Renewable energies attract more and more attention, since they address two major global problems: the acute increase in petrol price and the emission of carbon dioxide from fossil sources, one of the greenhouse gases (GHG) involved in climate change. The European Union (EU) directive on renewable energy [1] aims to enlarge the contribution of renewable energy sources to the total energy mix to up to 20%. Eurostat documented a gain of renewable energy in gross final energy consumption from 8.9% in 2006 to 10.3% in 2008 [2]. Among available renewable resources, the conversion of biomass into energy through the anaerobic digestion process has drastically increased in Europe [3]. In March 2007, EU leaders endorsed the Commission's roadmap on renewable energy and signed up to the energy plan of a 20% target for renewables in the EU's overall energy mix by 2020.

Bioenergy production is controversially discussed. During the global food crisis in 2008, prices for agricultural commodities increased dramatically, and the world public increasingly focused on energy crop production and related negative side effects. Especially in developing and newly industrializing countries often a mismatch in the usage of areas for food or bioenergy production can be observed, which gives rises to increasing costs for agricultural commodities, a loss in (semi-)natural areas, and a decrease in biodiversity [4,5]. Nevertheless, bioenergy production as renewable energy source is a valuable option to preserve fossil energy resources, as long as food production has priority and issues of nature conservation are adequately addressed. In the EU, biogas production from energy crops is increasingly important. Anaerobic digestion is a complex biological process through which organic polymers (polysaccharides, proteins, lipids) are degraded into biogas, the end product (reviewed by: [6–10]). Biogas is mostly composed of methane (CH_4) and carbon dioxide (CO_2) and trace compounds such as H_2S, NH_3, H_2O, and H_2 and can be converted into renewable energy (in Combined Heat and Power (CHP) units or by injection into the gas grid) and climate-neutral CO_2. In addition, the process by-product, namely the digestate (the undigested matter), is a mineral fertilizer substitute of excellent agronomic value, since it contains all the nutrients required for crop production [11,12].

The total biomass alone does not provide information about the total amount of energy that can be derived from the plants through anaerobic digestion, since this rather requires knowledge about substrate quality, its digestibility and the expected kinetics of its degradation during the anaerobic digestion process [8,9].

Biomethanation reactors have to be managed in a way that prevents acidosis (a microbial dysfunction caused by a drop of the pH well known to affect ruminal flora in dairy cattle, [12]), reduces feeding ration costs, maximizes methane production and profit, and prevents dysfunction. Therefore, for operators of biogas plants the true objective is to predict the substrate related BMP (and indirectly the digester performance). The conventional definition of the biomethane potential of an organic substrate is expressed as the normalized volume of methane produced per unit of organic total solid [14]. However, for the *in situ* approach presented in this study the biomethane potential (BMP) had to be related (a) to the field area (BMP_{area}) and (b) to the fresh biomass (BMP_{FM}). The BMP_{area} (in

units normal m^3 biogas per hectare, Nm^3/ha) strongly depends on total available biomass, whereas the substrate related potential, BMP_{FM} (in units normal m^3 biogas per ton fresh matter, Nm^3/t FM) rather relies on dry matter content and substrate composition. A normal cubic meter (Nm^3) is the metric expression of gas volume at standard conditions, and it is defined as being measured at 0 °C and 1 atmosphere (1,013 mbars) of pressure.

Anaerobic digestion is described in several phases involving four major groups of facultative or strict anaerobic microorganisms (hydrolyzing microorganisms, acidogenic bacteria, acetogenic bacteria, and methanogens) [8,9]: The production of CH_4 depends on the composition of the organic matter; lipids, for instance, produce more CH_4 than proteins and carbohydrates [8,9,15,16], and the chemical composition of crops significantly changes over time [17]. Thus, the BMP_{FM} varies among substrates between and within different plant species [14].

Determination of BMP_{FM} is usually carried out through substrate analysis that typically requires a digestion test elapsing over a minimum of 30 days using traditional laboratory methods [18] that rely on anaerobic digestion. This strongly restricts the number of substrate samples that can be analyzed and hinders to map the BMP_{FM} in spatially distributed regionalized assessments. Recently, Mayer *et al.* [14] suggested near infrared spectroscopy (NIRS) as an alternative technique to determine the BMP_{FM}. NIRS is widely used in feed and food quality monitoring [19–26] and is accepted since many years as routine method for determining forage quality parameters of various crops. In the bioenergy sector NIRS has been applied to estimate sulphur content in biodiesel [27], for predicting digestibility of maize silage [28–30] and fermentation parameters of silages [31], and for the assessment of *in situ* degradability parameters of crude protein and dry matter characteristics [32,33].

Hyperspectral remote sensing allows transferring NIRS method from the laboratory to *in situ* conditions. This provides the possibility to derive spatially explicit information of energy crops on local and regional scales using airborne hyperspectral imaging systems such as HyMap [34] or APEX [35].

The present study addresses the following research questions:

(1) Is a spectroscopic method in combination with a multivariate statistical model a reliable alternative to classical analytical approaches using micro-digestion for BMP_{FM} estimation of different maize varieties in the laboratory?
(2) Can the laboratory spectroscopic approach be adopted towards *in situ* conditions to allow a regionalized BMP_{FM} assessment of maize crops based on airborne hyperspectral imaging data (HyMap)?
(3) Can also the BMP_{area} be retrieved from HyMap data that strongly relies on above ground biomass?

The study area is located in Luxembourg and covers an area of ~80 km^2, which is characterized by different soil types and maize varieties. Potentials and limitations of the suggested approach are discussed.

2. Study Site and Methods

2.1. Study Site

The study site of the 2010 field campaign is located northwestern of the city of Luxembourg (Figure 1). The sampling sites are orientated along the HyMap flight line from the small villages

Kehlen (49.67°N, 6.04°E) in the southeast to Useldange (49.768°N, 5.99°E) and Everlange 49.772°N, 5.96°E) in the north of the strip. Agriculture and forests dominate the land-use in the area. The terrain elevation varies from 367 m above sea level at Kehlen in the South, to 250 m at Useldange in the North (Figure 1).

Figure 1. Sampling sites and HyMap image stripe 2010.

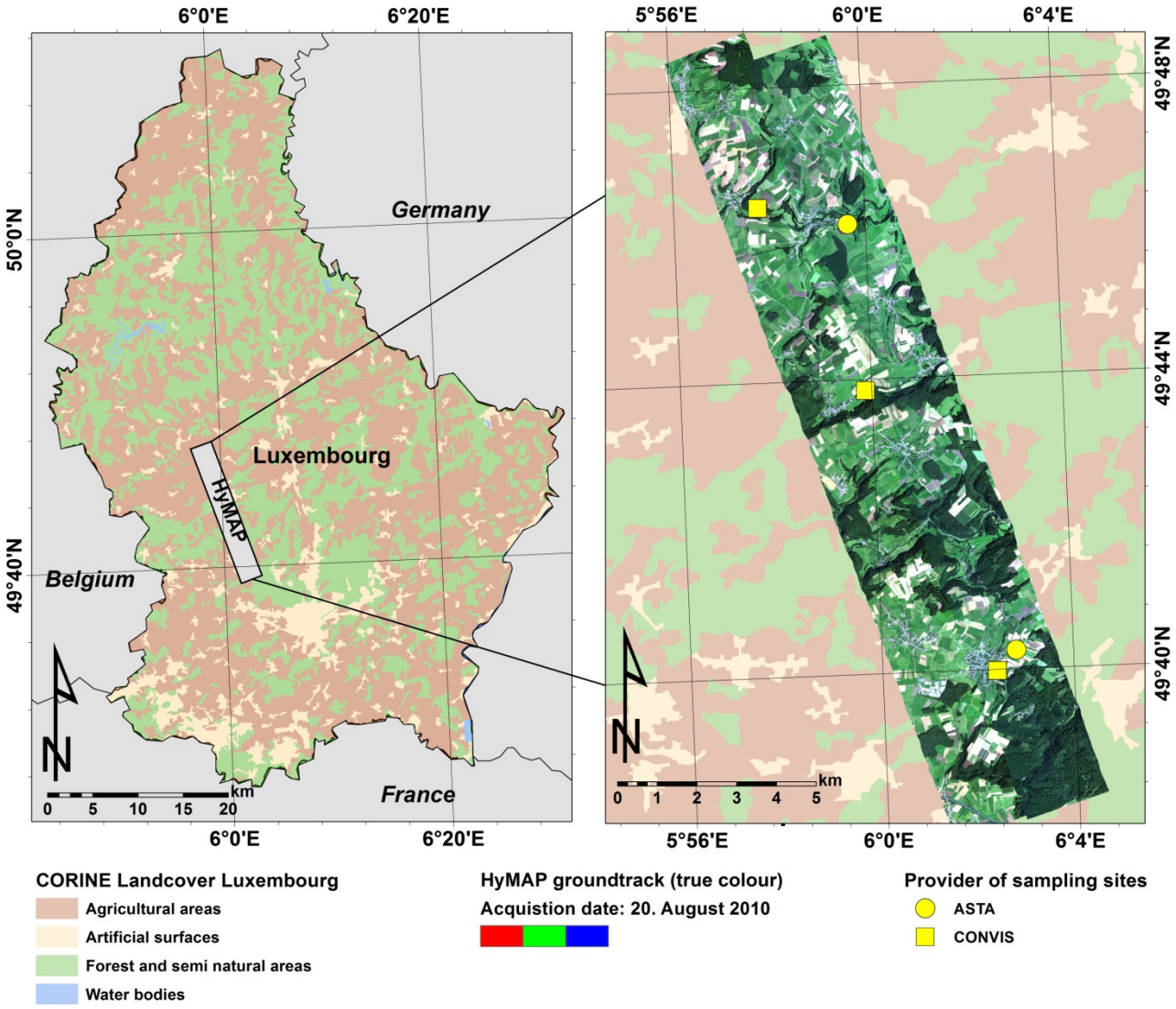

2.2. Methods

2.2.1. Acquisition of Airborne Hyperspectral HyMap Imaging Data

An overflight of the hyperspectral HyMap imaging sensor took place on 20 August 2010, approximately six weeks before the harvest date. The flight planning of the data provider did not allow capturing image data closer to the time of harvest. This caused a certain limitation for this study, as the maximum BMP levels of maize crops were not achieved at that time. HyMap provides 128 spectral bands across the reflective solar wavelength region (0.45–2.5 um) with bandwidths between 15 and 20 nm. According to the manufacturer the signal to noise ratio is >500:1 [34]. Geometrical and radiometrical corrections of the hyperspectral imagedata were carried out by the data provider, the

German Aerospace Center (DLR). Geometric correction of the data was performed by means of direct georeferencing (*i.e.*, direct measurements of the position and orientation of the sensor using differential GPS and Inertial Navigation System data) over a digital elevation model. The output grid contains position and viewing geometry parameters needed for the atmospheric correction. Atmospheric influences on radiances were then removed with the MODTRAN4 radiative transfer code [36]. Visibility and water vapor parameters of MODTRAN4 were estimated from the image itself using methods of Richter *et al.* [37] and Rodger and Lynch [38].

2.2.2. Field Campaign

The HyMap overflight was accompanied by an extended field campaign to collect reference data for the laboratory and *in situ* approach. The Administration des Services Techniques de l'Agriculture (ASTA, Luxembourg) has established two field trials within the HyMap flight line with different maize varieties. Additional maize fields within the flight line were provided by another agricultural organization in Luxembourg, the "CONVIS Herdbuch Service Elevage et Génétique". Twenty sub-plots within these fields were chosen as reference for statistical analysis in the *in situ* approach, resulting in a broad range of biomethane potentials. Within each field sampling plots of 4 × 4 m^2 were selected, according to the spatial resolution of HyMap. All sampling sites were geo-located through differential GPS (Trimble GeoXT GPS receiver with GeoBeacon) to enable their identification in the HyMap images. Analytical variables that were measured include leaf chlorophyll content, total biomass, BMP_{FM} and BMP_{area}. Total above ground biomass of each sub-plot was determined by shredding and weighting the whole maize plants using a self-propelled maize harvester (HALDRUP M-65, Inotec Engineering GmbH). BMP_{FM}, and BMP_{area} were determined after anaerobic digestion.

Table 1. Maize varieties considered in the study and number of available samples in the laboratory and *in situ* (HyMap) approaches.

Variety	Laboratory (Bruker MPA, FieldSpec 3MAX)	*In situ* (HyMap)
Unknown	15	14
P9578	2	2
INTENTION	1	1
HR 3400	1	1
FERNANDEZ	1	1
Piazza	2	
Seiddi CS	2	
Atletico	4	1
Graphic	1	
0808HYB	1	
Franki CS	1	
Aapple	2	
0945HYB	1	
Lucatoni	1	
	35	20

For the laboratory approach the number of BMP_{FM} reference samples could be increased by adding 15 additional (ensiled and vacuum packed)) silage maize samples to the calibration set that were already collected in October 2009 from other ASTA fields. This resulted in total in 35 calibration samples. Table 1 shows the maize varieties that were considered in the calibration set. Fifteen samples belong to unknown maize varieties.

2.2.3. Anaerobic Digestion

For BMP_{FM} determination the collected biomass samples were homogenized by shredding (1–2 cm particle size) and processed as silage until the substrate was stabilized through lactic fermentation (in about six weeks). Anaerobic digestion trials to determine the BMP_{FM} were carried out in three replicates in accordance with VDI ("Verein deutscher Ingenieure") 4630 [39] and DIN ("Deutsche Industrie-Norm") 38414 [40], that constitute German industrial analytical standards. The silage was filled into reactors of 2 liters total capacity filled with an inoculum (originating from a wastewater treatment plant) for anaerobic digestion. The total digestion process elapsed over 40 days. BMP_{area} was calculated by multiplying the BMP_{FM} with the fresh weight of the above ground biomass per hectare:

$$BMP_{area}[Nm^3/ha] = BMP_{FM}[Nm^3/t] \cdot biomass[t/ha] \quad (1)$$

2.2.4. Spectrometry and Partial least Square Regression

Two spectrometers were used for spectral BMP_{FM} estimation in the laboratory: The Bruker MPA and the ASD FieldSpec 3MAX. The Bruker MPA records reflectance in the NIR and SWIR spectral range (1,000–2,700 nm) at a mean spectral resolution of 2.15 nm. It uses an Integrating Sphere and an InGaAs detector. With this spectrometer, the silage samples were scanned in the spinning mode, covering a sample area of about 38 cm^2. The ASD FieldSpec 3MAX records reflectance with a spectral range from 400 to 2,500 nm and a sampling interval of 1.4 nm between 350 and 1,000 nm (using a 512 element Si-photodiode) and 2 nm between 1,000 nm and 2,500 nm (using a TE-cooled InGaAs-photodiode). Its spectral resolution is coarser compared to the Bruker MPA (3 nm FWHM (Full-Width Half-Maximum) @ 700 nm; 10 nm FWHM @ 1,400 nm; 10 nm FWHM @ 2,100 nm). The portable ASD instrument was included in the laboratory study for comparative purposes only, as it is widely used in the remote sensing community for *in situ* ground truth reflectance measurements. Unfortunately, the FieldSpec 3MAX was not available in the field campaign to capture above canopy reflectance data for a direct comparison with respective HyMap spectra. Figure 2 shows the difference in the spectral response of a maize silage sample (measured in the laboratory using the FieldSpec 3MAX and Bruker MPA) and the airborne above canopy signal (using the HyMap sensor). The reflectance curves of silage and fresh vegetation mostly differ in the VIS and NIR spectral regions. This is due to the decomposition of pigments during the silage process, especially the transformation of chlorophyll into phaeophytines, chlorophyllides, and phaeophorbides [41]. Furthermore, the destruction of cell structure alters the absorption along the NIR-plateau and modifies the shape of the red edge spectral region compared to healthy plant material. The main pigment in silage is phaeophytin, a derivative of chlorophyll that lacks a central Mg^{2+} ion. It is produced from chlorophyll through treatment with weak acids during fermentation in the silo [42].

Figure 2. Comparison of the spectra of the three spectrometers. ASD FieldSpec 3MAX (green dotted) and Bruker MPA (red dotted) spectra of one selected maize silage sample and an above canopy (airborne) HyMap reflectance curve for maize of August 2010 (blue).

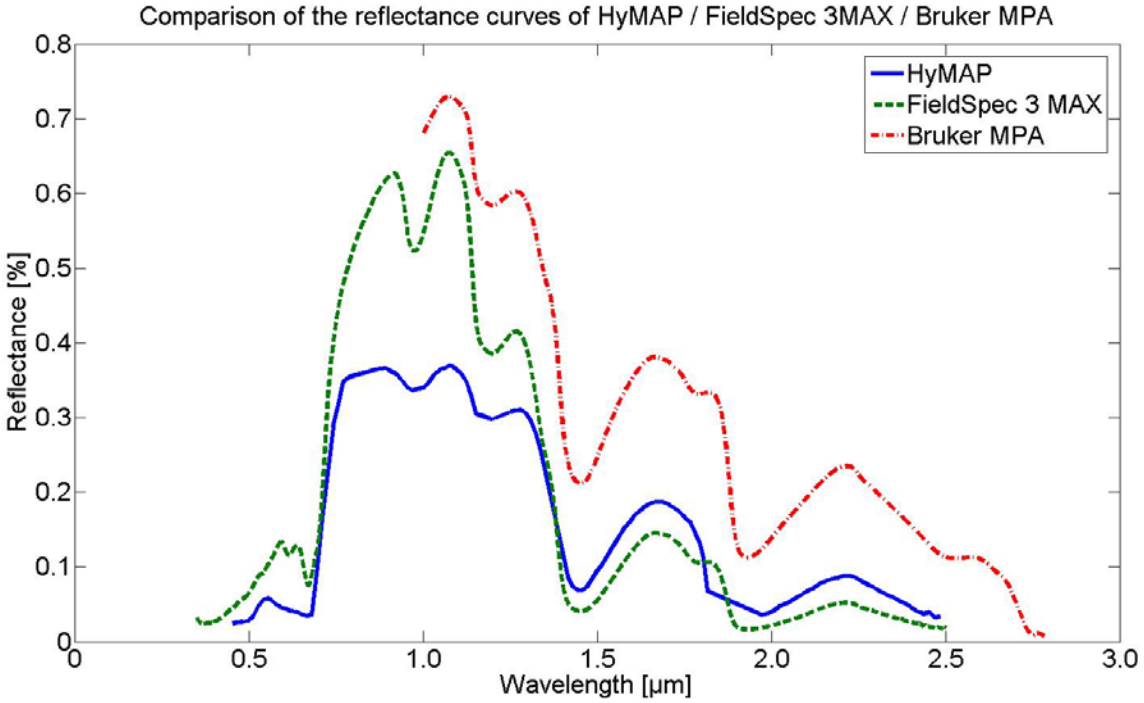

The recorded silage reflectance in the NIR and SWIR spectral region was found to be systematically higher for the Bruker MPA compared to the ASD FieldSpec instrument. To eliminate such baseline effects and to pronounce subtle absorption features, a Savitzky-Goley filter was used to convert all reflectance data collected in the laboratory into first derivative spectra. PLSR performed better using normalized derivative spectra. To this end vector normalization was applied to ensure that the length of all vectors (first derivative spectra) equals one (the unit length):

$$v_{norm} = \frac{v}{||v||} \tag{2}$$

with: v = vector (spectrum),
v_{norm} = normalized vector,
$||v||$ = Length of the vector.

The spectral signature of the silage was captured before digestion using both spectrometers. The PLSR module of the project-R statistical software package was used to regress the spectral data against the analytical BMP reference data. PLSR can be understood as an extension of multiple linear regression and principal component regression, as it aims to maximize the covariance between the spectral matrix (X) and response variables (Y) by accomplishing Eigen-decomposition of both matrices [43]. Leave-one-out cross-validation (CV) was used to test the predictive performance of the model and to identify a reasonable number of latent variables that provides good model generalization properties. Due to the unfavorable relation between the quantity of spectral points in the reflectance data and number of reference samples (35), it was observed that PLSR models tended to overfit. To remove unnecessary spectral information wavelengths with rank correlation coefficients <0.3 between

the spectral response variable and BMP reference data were excluded from the analysis. This threshold was also identified by leave-one-out cross-validation by systematically testing PLSR with different thresholds within the [0, 1] range.

BMP estimations in the *in situ* approach are based on above canopy reflectance and not from silage reflectance. Related spectral data in the HyMap image were selected from the closest possible distance to the differential GPS sampling points (biomass samples).

Since in the *in situ* approach the available calibration data set (n = 20) was rather small in comparison to the laboratory setup (n = 35), in addition Monte-Carlo simulations were carried out to assess the impact of different subsets on the model quality. To this end 200 times random training sample sets (n = 15) were selected from the available (*in situ*) reference data, following PLSR model calibrations for BMP_{FM} and BMP_{area} prediction and leave-one-out cross-validation. The multiple Pearson correlation coefficients were used to evaluate the predictions from each model.

3. Results

Table 2 depicts the correlation matrix among the considered variables. Obviously BMP_{FM} and BMP_{area} are not correlated with each other (r = 0.03), as both measures represent different information. As expected BMP_{area}, which is the methane yield per hectare, is mainly determined by variations in total available biomass (fresh matter, r = 0.97). Thus, total above ground biomass of maize is an adequate proxy for BMP_{area}. In contrast the BMP_{FM} is not correlated with total biomass (r = 0.06). This energy potential is expressed per unit weight biomass and is rather determined by substrate specific biochemical properties, such as lipids, proteins, and carbohydrates, and the dry matter content [8,9].

Table 2. Correlation matrix of maize sample characteristics in the *in situ* approach (samples of locations that were covered by HyMap data, n = 20).

	Biomass (t/ha)	**BMP_{FM} (Nm^3/t FM)**	**BMP_{area} (Nm^3/ha)**
Biomass (t/ha)	1.00**		
BMP_{FM} (Nm^3/t FM)	0.06	1.00**	
BMP_{area} (Nm^3/ha]	0.97**	0.03	1.00**

** Significant at 95% confidence level.

3.1. Spectral BMP_{FM} Estimation at Laboratory Scale

An ASD FieldSpec example first derivative spectrum is shown for one selected maize silage sample in Figure 3.

Most distinct features in the first derivative spectra are the red edge spectral region between 0.7 and 0.8 µm and the water absorption bands around 1.2 µm, 1.4 µm and 1.9 µm. The water bands are also clearly visible in the loading and regression vectors from the BMP_{FM}-PLSR prediction models (Figure 4).

Figure 3. Vector-normalized example first derivates spectrum of the ASD FieldSpec 3MAX of a maize silage sample.

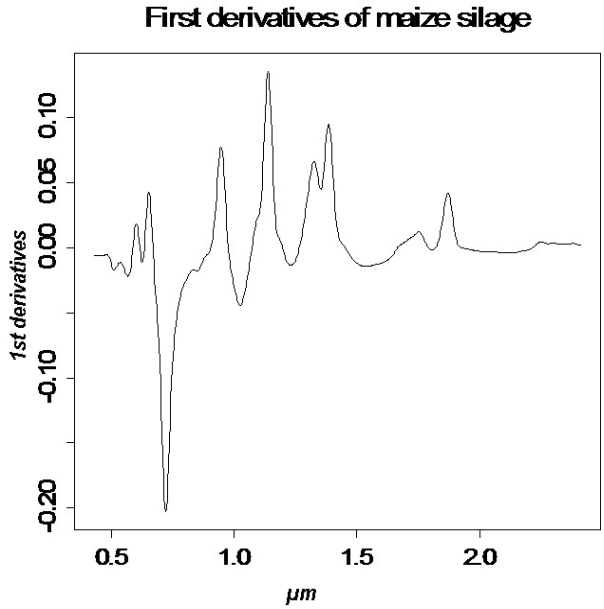

Figure 4. (**Right**) First two latent PLS loading vectors and explained variance using Bruker MPA spectra for BMP_{FM} prediction. The loadings represent the correlation between a latent PLS variable and spectral information. (**Left**) corresponding PLSR regression vector, which represents the weights that PLSR assigns to each wavelength for BMP_{FM} prediction.

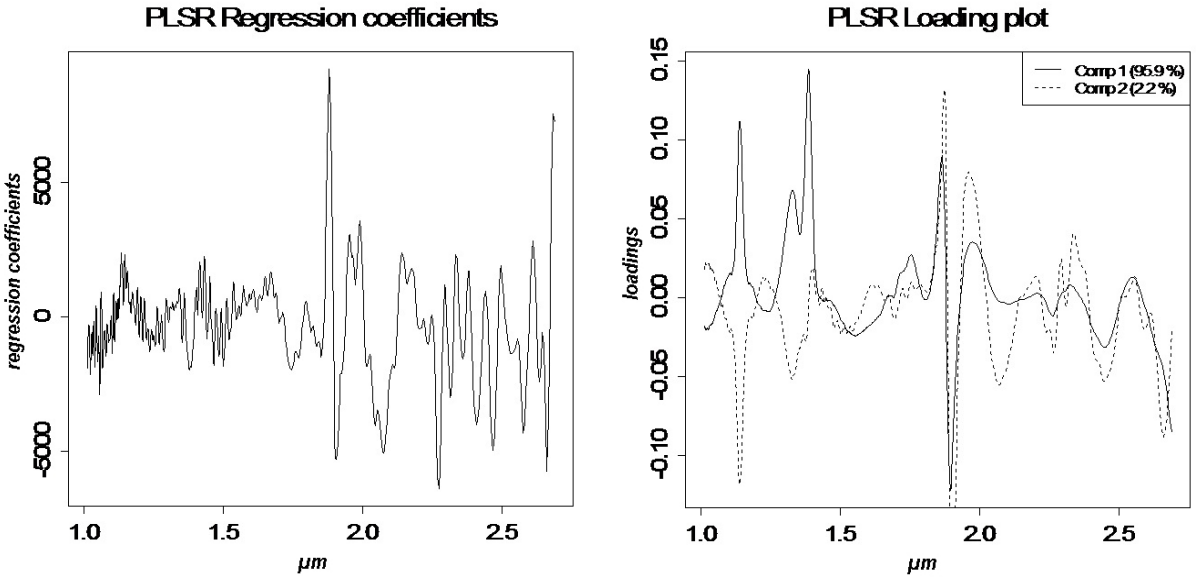

In the laboratory approach two PLSR models for BMP_{FM} estimations were calibrated using the Bruker MPA and the FieldSpec 3MAX normalized first derivative spectra. The loading plot of the respective Bruker MPA based PLSR prediction model is shown in Figure 4 and demonstrates that the first PLSR factor already explains the majority of the total variability of both, the independent variables X (the normalized derivative spectra, 95.9% explained variability) and the dependent

variable Y (the BMP_{FM}, 70% explained variability). The final cross-validated PLSR prediction model comprised 10 latent variables.

Cross-validated BMP_{FM} estimates are reliable using Bruker MPA spectra (r^2_{cv} = 0.82, n = 35, Figure 5) and confirm the potential of the spectroscopic method as a promising alternative to costly micro-digestion. Figure 5 suggests a linear relationship in estimated and analyzed BMP_{FM} values both between and within the considered maize varieties, but there appears a distinct variability at lower BMP_{FM} levels between 120 and 190 (Nm^3/t FM). The total BMP_{FM} range of the considered maize samples comprised 120 to 280 (Nm^3/t FM). The former sub-group solely represents the reference samples that were collected during the HyMap campaign in August 2010. The comparably low BMP_{FM} levels in this group can be explained by the early field campaign approximately six weeks before harvest date. In the mature crop state the BMP_{FM} is higher (>190 Nm^3/t FM) and driven by an increasing dry matter fraction of the total above ground biomass.

Figure 5. Crossvalidated (CV) results for BMP (Nm^3/t FM) estimation using ASD FieldSpec 3MAX spectral data (full spectral range). (**Left**) shows the results for the full calibration set (n = 35); (**Right**) depicts BMP_{FM} predictions after presenting group averaged spectra (n = 14) to this model.

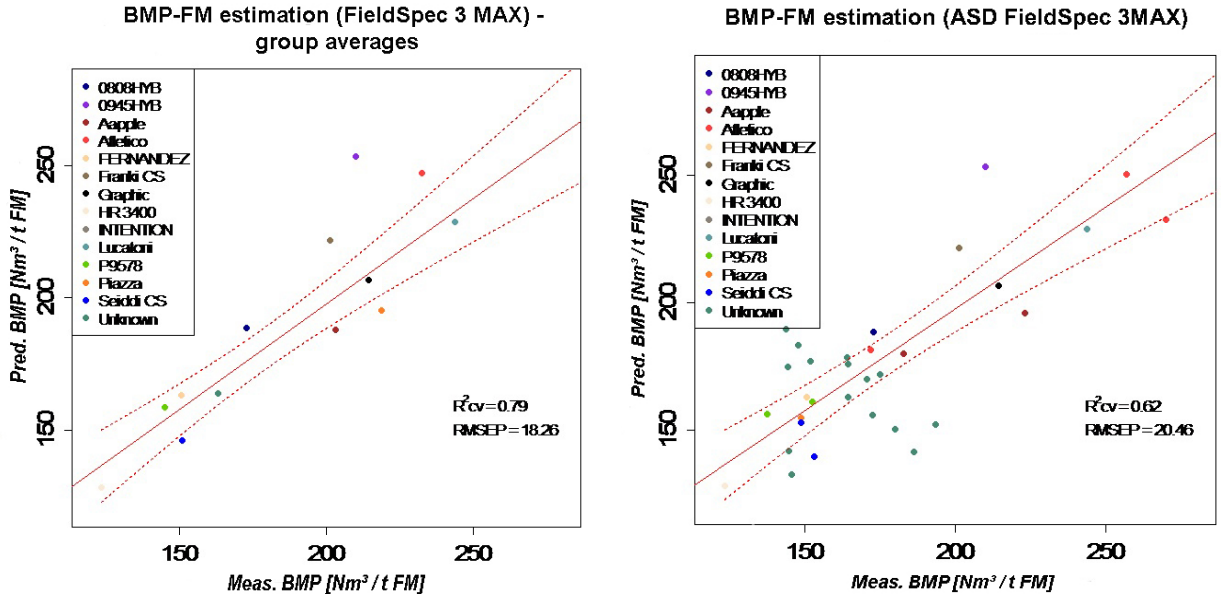

When group (variety) averaged derivative spectra are presented to the calibrated PLSR model (Figure 6), the explained variance increases (R^2_{cv} = 0.92). This suggests that the between-variety variance is better captured by the model than within group variability, although there is evidence from Figure 6(left) that also within several varieties a statistical relationship between BMP_{FM} and spectral response exists.

Figure 5(left) shows crossvalidated BMP_{FM} predictions using the PLSR model that was calibrated with ASD FieldSpec 3MAX data, that cover the full VIS/NIR/SWIR range. The related model comprised nine latent PLS factors in total.

Obviously, FieldSpec 3MAX based BMP_{FM} estimates are not as reliable as those obtained with the Bruker MPA instrument, despite the broader wavelength range of the ASD spectrometer. The

explained variability in the analyzed BMP_{FM}-values (R^2_{cv} = 0.62) is less compared to the Bruker MPA based model and the root mean squared error of prediction (RMSEP) is larger (11.81 (Nm^3/t FM) for the Bruker MPA and 24.24 (Nm^3/t FM) for the ASD FieldSpec, respectively). The BMP_{FM} prediction accuracy significantly improves when group mean averaged FieldSpec 3spectra are presented to the related model (R^2_{cv} = 0.78, Figure 6(right)). This suggests that also in this case the model is mainly driven by spectral differences between maize varieties. A distinct scattering in the BMP_{FM} estimates within the different maize varieties is obvious in Figure 5, too.

Figure 6. Crossvalidated (CV) results for BMP_{FM} (Nm^3/t FM) estimation using Bruker MPA spectral data and PLSR. The left figure shows the results for the full calibration set (n = 35); the right figure depicts BMP_{FM} predictions after presenting group averaged spectra (n = 14) to this model.

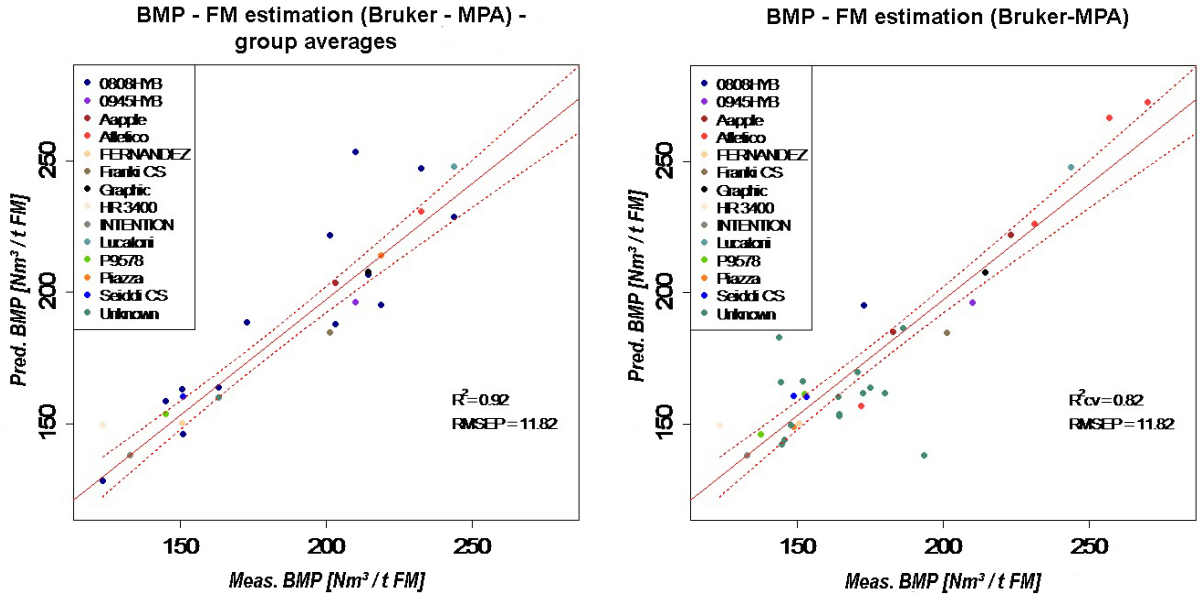

3.2. Remote Sensing Based BMP_{FM} Assessment

The aim of the *in situ* approach was the retrieval of the biomethane potential directly from above canopy reflectance (compare Figure 2) using of airborne HyMap data, instead of using maize silage spectra. A drawback in this approach was that here only a sub-sample from the calibration set of the laboratory approach was available for model calibration (n = 20) with rather small corresponding BMP_{FM} values (<190 (Nm^3/t FM)).

Figure 7 depicts crossvalidated PLSR estimations for BMP_{FM} (left) and BMP_{area} (right). Obviously, there exists a linear statistical relationship between HyMap spectra and the biomethane potential (R^2_{cv} = 0.52 for BMP_{FM} and R^2_{cv} = 0.23 for BMP_{area}); however, calibration errors are larger compared to the lab results and results for BMP_{area} are poor. The low BMP_{FM} levels in the calibration data set could be identified as major reason for the lower prediction accuracies: a PLSR-model calibrated with the same subset of 20 samples but using Bruker MPA spectra results in even worse BMP_{FM} estimates (R^2_{cv} = 0.34). Also the smaller calibration set (n = 20) in comparison with the lab approach (n = 35) contributes to the standard error of the regression coefficients.

Figure 7. Crossvalidated (CV) BMP_{FM} (**left**) and BMP_{area} (Nm^3/ha) (**right**) estimations using airborne hyperspectral HyMap imaging data.

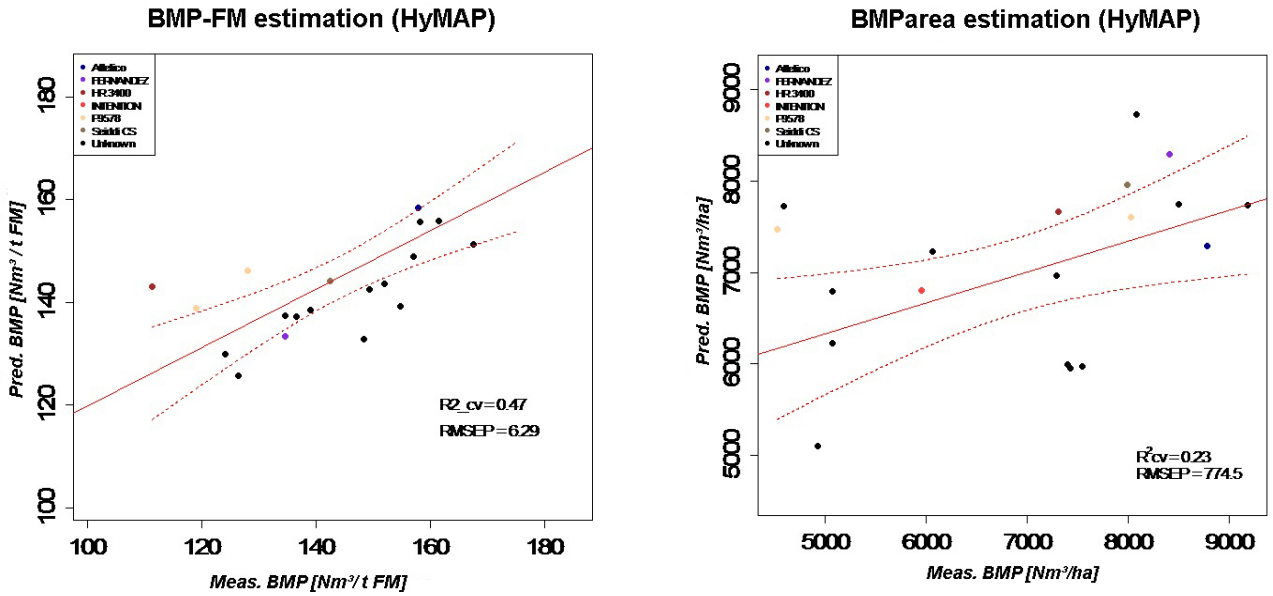

To assess in more detail, Monte-Carlo simulations were carried out. Figure 8 depicts the corresponding R_{cv}-histograms derived from each prediction model, which both are broadly and unimodally shaped. The respective R_{cv}-values range from 0.1 to 0.9 and thus clearly demonstrate a strong influence of the training data set composition on PLSR model quality. On the other hand, the R_{cv}-majority classes for BMP_{FM} (R_{cv} = 0.6–0.7) and BMP_{area} (R_{cv} = 0.4–0.5) correspond as expected well with the PLSR-model results shown in Figure 7 that are based on all available reference data in the *in situ* approach (n = 20).

Figure 8. Monte-Carlo simulation to estimate BMP_{FM} (left) and BMParea (right) from HyMap reflectance data using a limited training data set: 200 times subsamples (n = 15) were randomly selected from the total available reference data set in the *in situ* approach (n = 20) to assess the variability in the prediction accuracy (represented by cross-validated Pearson correlation coefficients).

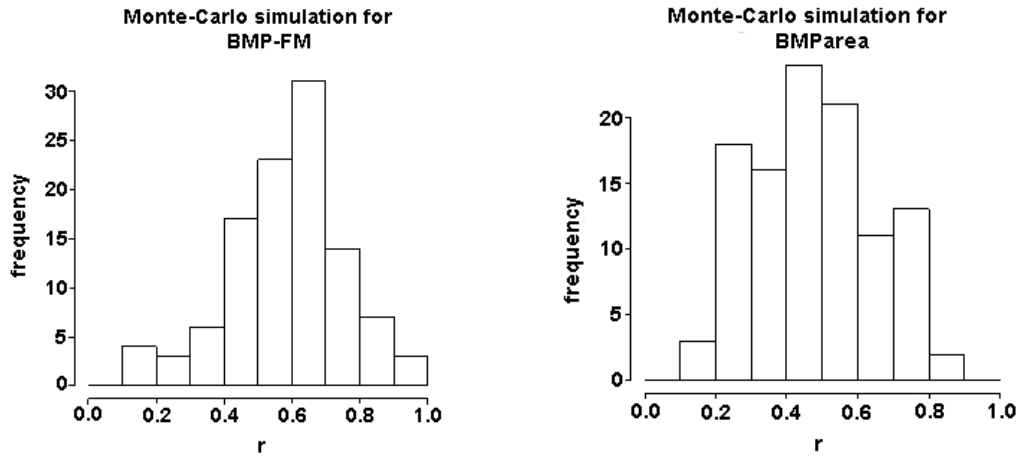

Figure 9 shows a map with spatially distributed BMP_{FM} estimates for maize fields in the study area after presenting the calibrated PLSR model to the HyMap image data. Coordinates of maize fields were taken from the annual agricultural cadastral map (2010) published by the Luxembourg administration. Estimated BMP_{FM} values vary between 40 and 170 (Nm^3/t FM) and the respective histogram is unimodal but left skewed, with a modal class for BMP_{FM} values around 150 (Nm^3/t FM). The majority of maize fields within the HyMap flight line are characterized by BMP_{FM} levels between 130 and 160 (Nm^3/t FM), which is in line with the range in the available calibration set. The small subset in Figure 9 shows the experimental ASTA test side near the village Kehlen from which the reference samples were taken in 2010 and that was characterized by a high variability of maize trials and varieties.

Figure 9. Regionalized BMP_{FM} estimation for maize fields in the study area using HyMap data (August 2010).

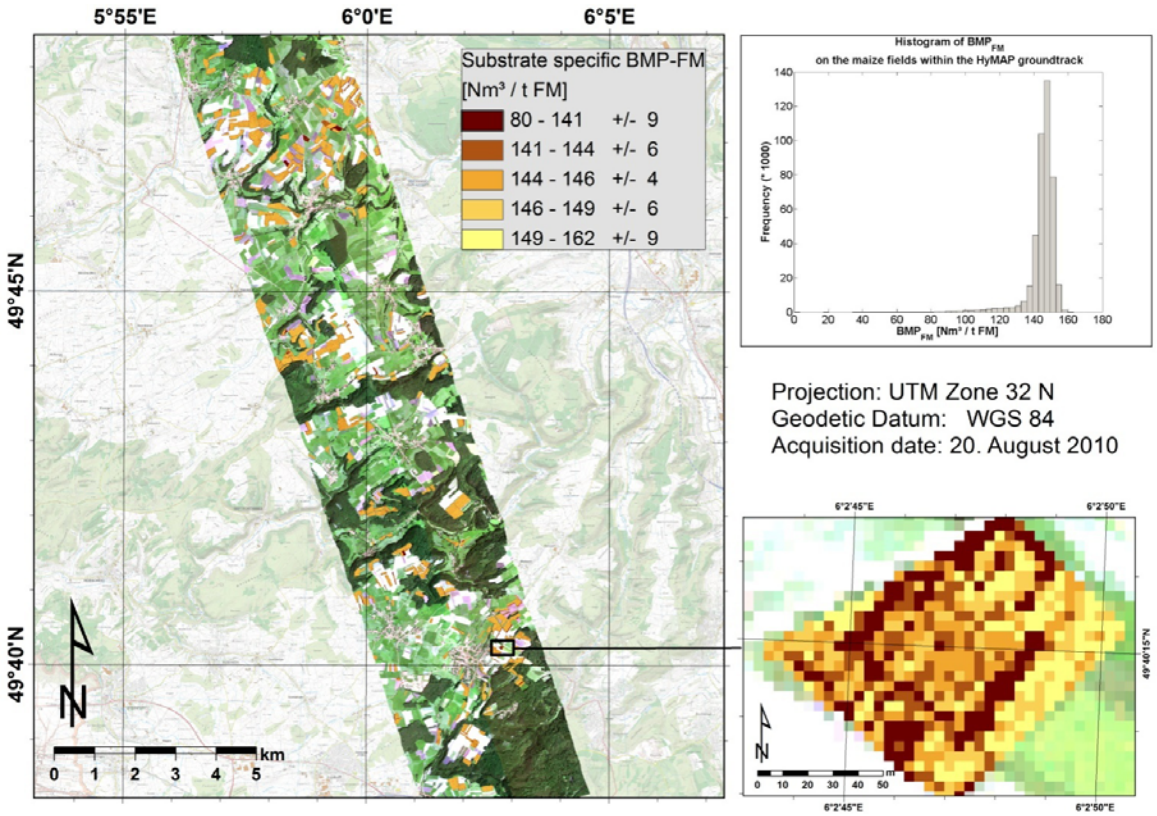

No BMP_{area} biomass map was created due to the poor prediction qualities of the respective PLSR-model. Also an attempt to retrieve total biomass of maize crops from the HyMap data resulted in poor PLSR-calibration statistics ($R^2_{cv} = 0.25$).

4. Discussion

The results from the laboratory approach demonstrate that NIRS is a reliable alternative to classical BMP_{FM} analysis [14,30], which does not rely on time consuming and expensive fermentation in micro-digesters, and that probably also works for other energy crops, such as rapeseed, miscanthus or

grassland. However, estimates in the *in situ* approach were of minor quality compared to the lab results ($R^2 = 0.51$).

The spectroscopic method uses indirect correlation between optically active biochemical properties (such as lignin, protein, cellulose *etc.*), which determines both $BMP_{FM,}$ and the spectral response of the substrate. Apart from the dry matter content is the composition of fibers among the key elements that determine the BMP_{FM} of organic substrates from agricultural origin: Lignin is the indigestible fraction of the cell wall component of plants. On the contrary, cellulose and hemicellulose are completely digestible if not inserted with lignin bounds [18].

BMP_{FM} retrievals at laboratory scale were most successful using the Bruker MPA instrument ($R^2_{cv} = 0.82$). The respective model was based on a rather small calibration set (n = 35), due to the time and costly fermentation trials using micro-digestion that hindered to collect more BMP reference data. For a profound NIRS calibration a larger calibration set will be necessary that takes into account more maize varieties and the full range of expected BMP_{FM} data.

The FieldSpec 3MAX instrument has been included in this study for comparative reasons only, since it represents a widely used reference for remote sensing applications. The prediction accuracy of the respective PLSR-model was lower compared to Bruker MPA based BMP_{FM} estimates, despite of its broader available spectral wavelength range. This demonstrates that for BMP retrieval a high SNR and spectral resolution is more important than including the VIS spectral region in the analysis. A missing link in the present study was the non-availability of FieldSpec 3MAX spectra in the *in situ* approach to compare HyMap data with above canopy measurements in the field. This aspect will be addressed in a further study.

There is evidence from both laboratory and *in situ* approaches (Figures 5 and 6) that the spectroscopic BMP_{FM} determination works best at higher BMP_{FM} levels > 180 (Nm^3/t FM) and related high dry matter fractions of the total biomass at the time of harvest. Reference data in the *in situ* approach derived from a point in time approximately six weeks before harvest, and consequently the full BMP_{FM} levels of the maize crops were not achieved, due to a lower dry matter content. There is evidence that the distinct variability in the dry matter contents at that time strongly affects the spectroscopic BMP_{FM} predictions. Also in the laboratory approach the quality of the related PLSR model declined when only related silage spectra of the field campaign samples were used for model calibration. (R^2 drops from 0.82 using the full calibration set to 0.34 using solely samples from the field campaign). The impact of variable dry matter contents on spectroscopic BMP_{FM} predictions needs to be further evaluated, but it is known from the literature that lower methane yield at an earlier stage in the vegetation growth cycle goes along with lower dry matter contents [17]. This variability and not the fact that above canopy spectra were used instead of silage spectra explains the weaker performance of *in situ* PLSR models compared to the lab approach.

Thus, it can be expected that *in situ* estimations will improve if hyperspectral remote sensing data closer to the date of harvest of maize crops are acquired, when both dry matter content and BMP_{FM} are at the maximum [17]. The *in situ* model in this study represents rather BMP_{FM} differences between maize varieties than within varieties. In 2010, 135 different maize varieties were grown up in Luxembourg (personal communication by ASTA, Luxembourg). In view of this variability it seems to be justified to suggest the presented method for the analysis of a spatial distributed BMP_{FM}.

The assessment of the area-based, regionalized potential (BMP_{area}) is only feasible at field conditions. In general, the strong positive correlation between BMP_{area} and biomass (Figure 2(left)) allows estimating the former directly from the latter using a linear regression model. However, in the present study neither the retrieval of total biomass from HyMap data, nor a direct estimation of the BMP_{area} from HyMap data (R_{cv}^2 = 0.23, RMSE = 801.76 Nm^3/ha) was successful. The BMP_{area}-model lacks from the tendency to overestimate measured BMP_{area} at lower ranges (5,000–6,000 Nm^3/ha), whereas BMP_{area} at higher levels (8,000–9,000 Nm^3/ha, compare Figure 9) are underestimated. Nevertheless, the strong correlation between BMP_{area} and total biomass provides the opportunity to estimate this potential directly from total biomass, and in fact there exist many case studies, where biomass has been successfully retrieved from crops using remote sensing techniques (e.g., [44–46]). Alternative biomass (and thus BMP_{area}) assessment approaches are based on crop modeling techniques and on the concept of the *biomass potential*. The *biomass potential* is either derived from production data combined with assumptions of percentage of residues from agricultural and forestry products, or from statistical data combined with assumptions of crop specific quantities of residue per area unit [47–50]. The *biomass potential* can be further divided into the *theoretical total biomass potential,* which is an estimate of the standing biomass based on calculation or measurement of the net primary productivity of a biome [51], and the *technical biomass potential* that is subject to the available technology (harvest, collection, amount of residues, *etc.*) [52,53]. On the other hand, deterministic crop growth models aim at estimating the total biomass amount as function of several abiotic factors (weather, soil type), farm management (soil tillage, planting density, sowing date, weeding intensity, fertilizer rates, crop protection against pests and diseases, harvest techniques, post-harvest losses, degree of mechanization), land development (field size, terracing, drainage, irrigation) and socio-economic drivers [54–57].

5. Conclusions

The aim of this study was the retrieval of the biomethane potential using NIRS and hyperspectral remote sensing. The results underline the potential of the spectroscopic BMP_{FM} method as a cheap and fast alternative to fermentation analysis in micro-digesters in the laboratory (R^2_{cv} = 0.82), and demonstrate the potential of hyperspectral remote sensing for spatially distributed BMP retrievals (R^2_{cv} = 0.47). There is evidence that the remote sensing method only works reliably close to the time of harvest, when the dry matter content is at its maximum and becomes less variable. Considering recent and forthcoming airborne and satellite based hyperspectral sensors, for instance the German EnMAP-mission, the method has the potential to provide stakeholders with a spatial estimation of the crop yield and the related BMP_{FM} before harvesting energy crops. On the other hand near sensing techniques could profit from this method as well; spectrometers can be mounted on reaping machines to assess substrate quality and BMP_{FM} of shredded plant material "on the fly". The second goal of this study, the regional estimation of the BMP_{area} of maize crops, could not be achieved (R_{cv}^2 = 0.23). The BMP_{area} is closely related to the total biomass of energy crops, but only a weak correlation between HyMap- and above ground biomass data could be found (R^2_{cv} = 0.25). This opens the opportunity for alternative techniques for regional biomass and thus also BMP_{area} assessments, such as assimilation of remote sensing data in deterministic crop models to better represent spatial heterogeneity in such modeling approaches.

Acknowledgements

We would like to thank the FNR (Fonds National de la Recherche, Luxembourg, projects HYPERSPEC C09/SR/21, BIONIR CO8/SR/13, and SOC3D INTER/STEREOII/10/01) and the BMWi (Bundesministerium für Wirtschaft, Germany) (project EnMAP-BMP 50 EE 1021) for funding this study. We are especially thankful for the good collaboration with ASTA and CONVIS and their support in providing reference samples for spectroscopic analysis. The technical support of Anaïs Noo, Sébastien Lemaigre, Bénédicte De-Vos and Elodie Boland for the BMP analyses is also greatly acknowledged.

References

1. EU Directive 2009/28/EC of the European Parliament and of the Council of 23 April 2009 on the Promotion of the use of energy from renewable sources and amending and subsequently repealing Directives 2001/77/EC and 2003/30/EC. Available online: http://eurlex.europa.eu/LexUriServ/LexUriServ.do?uri=Oj:L:2009:140:0016:0062:en:PDF (accessed on 14 January 2013).
2. Roubanis, N.; Dahlström, C.; Noizette, P. *Eurostat—Statistics in Focus 56/2010, Environment and Energy, Renewable Energy Statistics*; 2010; p. 2. Available online: http://epp.eurostat.ec.europa.eu/cache/ITY_OFFPUB/KS-SF-10-056/EN/KS-SF-10-056-EN.PDF (accessed on 24 April 2011).
3. Biermayr, P.; Cremer, C.; Faber, T.; Kranzl, L.; Ragwitz, M.; Resch, G.; Toro, F. *Bestimmung der Potenziale und Ausarbeitung von Strategien zur verstärkten Nutzung von erneuerbaren Energien in Luxemburg. Fraunhofer Institut für System- und Innovationsforschung (Fh-ISI)*; Energy Economics Group TU Wien/BSR-Sustainability: Luxemburg/Karlsruhe, Germany, 26 March 2007. Available online: http://www.eco.public.lu/salle_de_presse/com_presse_et_art_actu/2007/03/26_energies/endbericht.pdf (accessed on 14 January 2013).
4. Singh, S. Global food crisis: Magnitude, causes and policy measures. *Int. J. Soc. Econ.* **2009**, *36*, 23–36.
5. Atzberger, C. Advances in remote sensing of agriculture: Context description, existing operational monitoring systems and major information needs. *Remote Sens.* **2013**, submitted.
6. Chynoweth, D.; Isaacson, R. *Anaerobic Digestion of Biomass*; Elsevier Applied Sciences: London, UK/New York, NY, USA, 1987; p. 279.
7. Malina, J.F.; Pohland, F.G. *Design of Anaerobic Processes for the Treatment of Industrial and Municipal Wastes*; CRC Press: Boca Raton, FL, USA, 1992; Volume 7, p. 214.
8. Ahring, B.K. *Biomethanation I.* (*Advances in Biochemical Engineering Biotechnology)*, 1st ed.; Springer-Verlag: Berlin/Heidelberg, Germany/New York, NY, USA, 2003; p. 220.
9. Ahring, B.K. *Biomethanation II. Advances in Biochemical Engineering Biotechnology*, 2nd ed.; Springer-Verlag: Berlin/Heidelberg, Germany/New York, NY, USA, 2003; p. 212.
10. Gerardi, M.H. *The Microbiology of Anaerobic Digesters (Waste Water Microbiology Series)*; John Wiley & Sons, Inc.: Hoboken, NJ, USA, 2003; p. 177.

11. Birkmose, T. Digested Manure is a Valuable Fertiliser. The Future of Biogas in Europe III. In *Proceedings of an EC-Sponsored PROBIOGAS Conference*, Esbjerg, Denmark, 27 June 2007; p. 91.
12. Palm, O. The Quality of Liquid and Solid Digestate from Biogas Plants and its Application in Agriculture. In *Proceedings of ECN/ORBIT e.V. Workshop-The Future for Anaerobic Digestion of Organic Waste in Europe*, Wageningen, The Netherlands, 13 October 2008; Nr. 20, 2008.
13. Plaizier, J.C.; Krause, D.O.; Gozho, G.N.; McBride, B.W. Subacute ruminal acidosis in dairy cows: The physiological causes, incidence and consequences. *Vet. J.* **2008**, *176*, 21–31.
14. Mayer, F.; Noo, A.; Sinnaeve, G.; Dardenne, P.; Hoffmann, L.; Flammang, J.; Foucart, G.; Gerin, P.; Delfosse, P. Evaluation of the Prediction of Biogas Production from Maize Silages with Near Infrared Spectroscopy (NIRS). In *Proceedings of the International Congress Progress: Biogas II*, Stuttgart, Germany, 30 March–1 April 2011; p. 235–240.
15. Buswell, A.M.; Müller, H.F. Mechanism of methane fermentation. *Ind. Eng. Chem.* **1952**, *44*, 550–552.
16. Boyle, W.C. Energy Recovery from Sanitary Landfills—A Review. In *Microbiol Energy Conversion*; Schlegel, H.G., Barnea, S., Eds.; Pergamon Press: Oxford, UK, 1976; pp. 119–138.
17. Schittenhelm, S. Chemical composition and methane yield of maize hybrids with contrasting maturity. *Eur. J. Agron.* **2008**, *29*, 72–79.
18. Delfosse, P.; Lemaigre, S.; Flammang, J.; Neuberg, C.; Hausman, J.F.; Hoffmann, L. Evaluation Variétale du Maïs, du Tournesol, et du Sorgho Pour la Méthanisation au Grand-Duché de Luxembourg (in German). In *Proceedings of a One Day Meeting on Biométhanisation Agricole at Redange*, Centre de Recherche Public-Gabriel Lippmann & Administration des Services Techniques de l'Agriculture: Luxembourg, 13 September 2007.
19. Hoffmann, R.M.; Wilson, J.A.; Kronfeld, D.S.; Cooper, W.L.; Lawrence, L.A.; Sklan, D.; Harris, P. Hydrolizable carbohydrates in pasture, hay, and horse feeds: Direct assay and seasonal variation. *J. Anim. Sci.* **2001**, *79*, 500–506.
20. Hollung, K.; Øverland, M.; Hrustic, M.; Sekulic, P.; Miladinovic, J.; Martens, H.; Narum, B.; Sahlstrøm, S.; Sørensen, M.; Storebakken, T.; Skrede, A. Evaluation of nonstarch polysaccharides and oligosaccharide content of different soybean varieties (*Glycine max*) by near-infrared spectroscopy and proteomics. *J. Agric. Food Chem.* **2005**, *53*, 9112–9121.
21. Kumagai, M.; Ohisa, N.; Amano, T.; Ogawa, N. Canonical discriminant analysis of cadmium content levels in unpolished rice using a portable near-infrared spectrometer. *Anal. Sci.* **2003**, *19*, 1553–1555.
22. Martens, H.; Næs, T. Multivariate Calibration by Data Compression. In *Near-Infrared Technology in the Agricultural and Food Industries*, 2nd eds.; Williams, P., Norris, K., Eds.; American Association of Cereal Chemists: St. Paul, MN, USA, 2001; pp. 59–100.
23. Satu, T. New estimation method for fatty acid composition in oil using near infrared spectroscopy. *Biosci. Biotechnol. Biochem.* **2002**, *66*, 2543–2548.
24. Park, R.; Agnew, R.E.; Kilpatrick, D.J. The effect of freezing and thawing on grass silage quality predictions based on near infrared reflectance spectroscopy. *Anim. Feed Sci. Technol.* **2002**, *102*, 151–167.

25. Tatavarti, A.S.; Fahmy, R.; Wu, H.; Hussain, A.S.; Marnane, W.; Bensley, D.; Hollenbeck, G.; Hoag, S.W. Assessment of NIR spectroscopy for nondestructive analysis of physical and chemical attributes of sulfamethazine bolus dosage forms. *AAPS Pharm. Sci. Tech.* **2005**, *6*, E91–E99.
26. Mentkink, R.L.; Hoffman, P.C.; Bauman, L.M. Utility of near-infrared reflectance spectroscopy to predict nutrient composition and *in vitro* digestibility of total mixed rations. *J. Dairy Sci.* **2006**, *89*, 2320–2326.
27. Galvão, H.R.K.; Araújo, M.C.U.; Silva, E.C.; José, G.E.; Soares S.F.C.; Paiva, H.M. Cross-validation for the selection of spectral variables using the successive projections algorithm. *J. Braz. Chem. Soc.* **2007**, *18*, 8.
28. Dardenne, P.; Andrieu, J.; Barriere, Y.; Biston, R.; Demarquilly, C.; Femenais, N.; Lila, M.; Maupetit, P.; Riviere, F.; Ronsin, T. Composition and nutritive value of whole maize plants fed fresh to sheep-II Prediction of the *in vivo* organic matter digestibility. *Ann. Zootech.* **1993**, *42*, 251–270.
29. De Boever, J.L.; Cottyn, B.G.; De Brabander, D.L.; Vanacker, J.M.; Boucque, C.V. Prediction of the feedingvalue of maize silages by chemical parameters, *in vitro* digestibility and NIRS. *Anim. Feed Sci. Technol.* **1997**, *66*, 211–222.
30. Lovett, D.K.; Deaville, E.R.; Moulda, F.; Givens, D.I.; Owen, E. Using near infrared reflectance spectroscopy (NIRS) to predict the biological parameters of maize silage. *Anim. Feed Sci. Tech.* **2004**, *115*, 179–187.
31. Sorensen, L.K. Prediction of fermentation parameters in grass and corn silage by near infrared spectroscopy. *J. Dairy Sci.* **2004**, *87*, 3826–3835.
32. Todorov, N.; Atanassova, S.; Pavlov, D.; Grigorova, R. Prediction of dry matter and protein degradability of forages by near infrared spectroscopy. *Livest. Prod. Sci.* **1994**, *39*, 89–91.
33. Walters, C.J.; Givens, D.I. Nitrogen degradability of fresh herbage: effect of maturity and growth type, and prediction from chemical composition and by near infrared reflectance spectroscopy. *Anim. Feed Sci. Technol.* **1992**, *38*, 335–349.
34. Cocks, T.; Jenssen, R.; Steward, A.; Wilson, I.; Shields, T. The Hymap Airborne Hyperspectral Sensor: The System, Calibration and Performance. In *Proceedings of the 1st EARSEL Workshop on Imaging Spectroscopy*, Zurich, German, 6–8 October 1998.
35. Schaepman, M. E.; de Vos, L.; Itten, K. I. APEX-airborne PRISM experiment: Hyperspectral radiometric performance analysis for the simulation of the future ESA land surface processes earth explorer mission. *Proc. SPIE* **1998**, *3438*, 253–262.
36. Berk, A.; Anderson, G.P.; Acharya, P.K.; Chetwind, J.H.; Bernstein, L.S.; Shettle, E.P.; Matthew, M.W.; Alder-Golden, S.M. *Modtran4 User's Manual*; Air Force Research Laboratory: Hanscom, MA, USA, 1999; p. 93.
37. Richter, R.; Schlapfer, D.; Muller, A. An automatic atmospheric correction algorithm for visible/NIR imagery. *Int. J. Remote Sens.* **2006**, *27*, 2077–2085.
38. Rodger, A.; Lynch, M.J. Determining Atmospheric Column Water Vapour in the 0.4–2.5 μm Spectral Region. In *Proceedings of the JPL-NASA AVIRIS Workshop 2001*, Pasadena, CA, USA, 27 February–2 March 2001.

39. Verein Deutscher Ingenieure. *VDI 4630-Fermentation of Organic Materials, Characterisation of the Substrates, Sampling, Collection of Material Data, Fermentation Tests*; VDI-Handbuch Energietechnik, Beuth Verlag GmbH: Berlin, Germany, 2006; p. 92.
40. Fachgrupe Wasserchemie in der Gesellschaft Deutscher Chemiker und Normausschuss Wasserwesen (NAW) im DIN Deutscher Institut für Normung e.V. DIN 38414-Bestimmung des Faulverhaltens (S8). In *Deutsche Einheitsverfahren zur Wasser-, Abwasser-, und Schlammuntersuchung. Physikalische, Chemische, Biologische und Bakteriologische Verfahren*; VCH Verlagsgesellschaft mbH: Weinheim, Germany, 1987.
41. Kowalewska, G.; Szymczak, M. Influence of selected abiotic factors on the decomposition of chlorophylls. *Oceanologia* **2001**, *43*, 315–328.
42. Woodman, H.E. The nature of the pigment of silage. *J. Agr. Sci.* **1923**, *13*, 240–242.
43. Wold, S.; Sjöström, M.; Eriksson, L. PLS-regression: A basic tool of chemometrics. *Chemometr. Intell. Lab. Syst.* **2001**, *58*, 109–130.
44. Cho, A.K.; Skidmore, M.A. Hyperspectral predictors for monitoring biomass production in Mediterranean mountain grasslands: Majella National Park, Italy. *Int. J. Remote Sens.* **2009**, *30*, 499–515.
45. Koppe, W.; Li, F.; Gnyp, M.; Miao, Y.; Jia, L.; Chen, X.; Zhang, F.; Bareth, G. Evaluating multispectral and hyperspectral satellite remote sensing data for estimating winter wheat growth parameters at regional scale in the North China plain. *Photogramm. Fernerkun.* **2010**, *3*, 167–178.
46. Darvishzadeh, R.; Skidmore, A.; Atzberger, C.; van Wieren, S. Estimation of vegetation LAI from hyperspectral reflectance data: Effects of soil type and plant architecture. *Int. J. Appl. Earth Obs. Geoinf.* **2008**, *10*, 358–373.
47. Ranney, J.W.; Cushman, J.H. Regional Evaluation of Woody Biomass Production for Fuels in the Southeast. In *Biotechnology and Bioengineering Symposium No. 10*; Wiley: New York, NY, USA, 1980; pp. 10–20.
48. Gehrung, J.; Scholz, Y. The application of simulated NPP data in improving the assessment of the spatial distribution of biomass in Europe. *Biomass Bioenerg.* **2009**, *33*, 712–720.
49. Phillips, V.D.; Liu, W.; Merriam, R.A.; Singh, D. Biomass systems model estimates of short-rotation hardwood production in Hawaii. *Biomass Bioenerg.* **1993**, *5*, 421–429.
50. Liu, W.; Merriam, R.A.; Phillips, V.D.; Singh, D. Estimating shortrotation *Eucalyptus saligna* production in Hawaii: An integrated yields and economic model. *Bioresour. Technol.* **1993**, *45*, 167–176.
51. Voivontas, D.; Assimacopoulos, D.; Koukios, E.G. Assessment of biomass potential for power production: a GIS based method. *Biomass Bioenerg.* **2001**, *20*, 101–112.
52. Milbrandt, A. *A Geographic Perspective on the Current Biomass Resource Availability in the United States*; Technical Report No. NREL/TP-560-39181; NREL: Golden, CO, USA, 2005. Available online: http://www.nrel.gov/docs/fy06osti/39181.pdf (accessed on 11 January 2013).
53. Beccali, M.; Columba, P.; D'Alberti, V.; Franzitta, V. Assessment of bioenergy potential in Sicily: A GIS–based support methodology. *Biomass Bioenerg.* **2009**, *33*, 79–87.

54. van Diepen, C.A.; van der Wal, T. Crop Growth Monitoring and Yield Forecasting at Regional and National Scale. In *Proceedings of Workshop for Central and Eastern Europe on Agrometeorological Models: Theory and Applications in the MARS Project*, Ispra, Italy, 21–25 November 1994; pp. 143–157.
55. Svendsen, H.; Hansen, S.; Jensen, H.E. Simulation of crop production, water and nitrogen balances in two German agro-ecosystems using the DAISY model. *Ecol. Model.* **1995**, *81*, 197–212.
56. Diekrüger, B.; Sönergerath, D.; Kersebaum, K.C.; McVoy, C.W. Validity of agroecosystem models—A comparison of results of different models applied to the same data set. *Ecol. Model.* **1995**, *81*, 3–29.
57. Wallach, D.; Makowski, D.; Jones, J. *Working with Dynamic Crop Models—Evaluation, Analysis, and Parameterization, and Applications*; Elsevier: Amsterdam, The Netherlands, 2006; p. 446.